

Supplementary Information

Concave gold nanocubes assemblies as nanotraps for surface-enhanced Raman scattering-based detection of proteins

Paolo Matteini^{1*}, Marella de Angelis¹, Lorenzo Ulivi², Sonia Centi³, Roberto Pini¹

1. Institute of Applied Physics "Nello Carrara", National Research Council
via Madonna del Piano 10, I-50019 Sesto Fiorentino, Italy
Fax: (+) 39 055 52255305
E-mail: p.matteini@ifac.cnr.it;
2. Institute for Complex Systems, National Research Council
via Madonna del Piano 10, I-50019 Sesto Fiorentino, Italy
3. Department of Biomedical, Experimental and Clinical Sciences, University of Florence, viale
Pieraccini 6, I-50139 Firenze, Italy

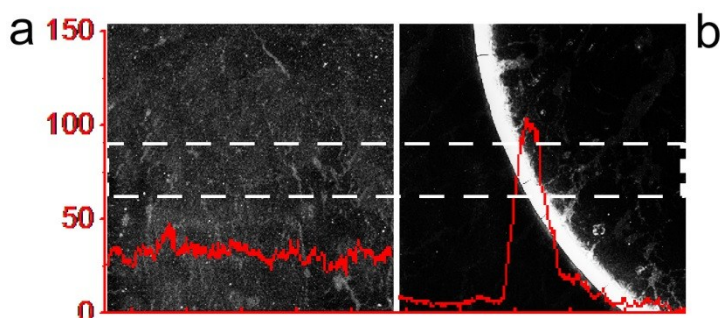


Fig. S1. Fluorescence images ($\lambda_{\text{ex}} = 488 \text{ nm}$, $2 \times 2 \text{ mm}^2$) of anti-rabbit IgG-FITC ($10 \mu\text{L}$, $2 \cdot 10^{-6} \text{ M}$) deposited over a CNCs-PDMS substrate according to the procedure described in Fig. 1 (a) and by drop deposition (b). The fluorescence intensity profile (red line, left y-axis, a.u.) of the protein averaged over the rectangular selection (indicated with a dashed line) is superimposed. The fluorescence signal is essentially constant throughout the sample when procedure (a) is used while is mainly localized at the edge of the dried drop and very low inside in the case of procedure (b).

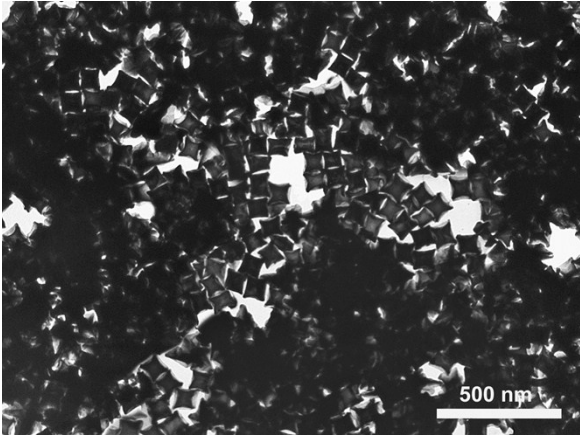


Fig. S2. TEM image of CNCs assembled by using 1 mM alkanethiol.

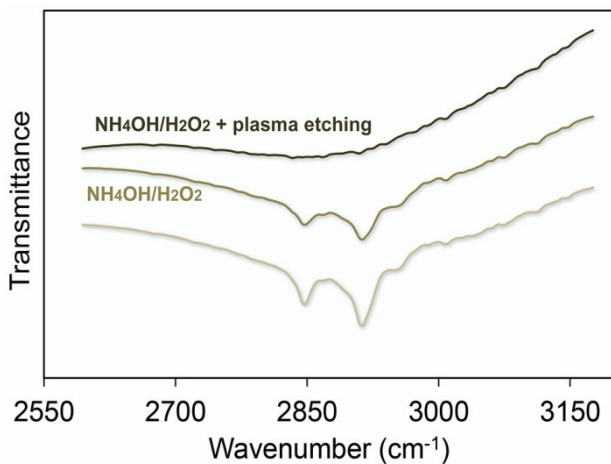


Fig. S3. ATR-FTIR spectra of CNCs-PDMS substrates: as-prepared (bottom), after the alkaline oxidizing treatment (middle) and further plasma oxygen cleaning (top). The disappearance of the 2846 and 2916 cm^{-1} bands assigned to the symmetric and asymmetric stretching CH_2 vibrations of the alkanethiol chain [A.N. Parikh and D.L. Allara, *J. Chem. Phys.* 1992, **96**, 927-945] suggests its complete removal [D.J. Kim, R. Pitchimani, D.E. Snow, L.J. Hope-Weeks, *Scanning*, 2008, **30**, 118-122] from the gold surface once the treatment was completed.

Calculation of the Enhancement Factor

The enhancement factor (EF) has been determined by comparing the 1594 cm^{-1} band intensity of the SERS spectrum (I_{SERS}) of 4-methylbenzenethiol (MBT) molecules deposited on CNCs substrates with that of the Raman measurement (I_{R}) of solid MBT. We have used the definition for the average SERS EF on substrates given by Le Ru *et al.* [E.C. Le Ru, E. Blackie, M. Meyer, P. G. Etchegoin, *J. Phys. Chem. C*, 2007, **111**, 13794-13803]:

$$EF = \frac{I_{\text{SERS}} / N_{\text{Surf}}}{I_{\text{R}} / N_{\text{Vol}}}, \quad (1)$$

Where N_{Surf} is the average number of adsorbed molecules in the scattering volume (i.e. at the SERS surface) for the SERS experiment, N_{Vol} is the average number of molecules in the scattering volume for the Raman measurement.

For the SERS measurement we assume the substrate consisting of a repeating pattern metallic structures and the irradiated area much larger than the individual structures forming the substrate. Let $\mu_M[\text{m}^{-2}]$ be the surface density of the individual nanostructures with respect to the main plane forming the substrate, and A_M the metallic surface area in each structure. Assuming a surface density of molecules $\mu_S[\text{m}^{-2}]$ on the metal (with footprint f_p being its reciprocal), if A_{eff} is the effective surface area of the scattering volume, we can define $N_{Surf} = \mu_M A_M \mu_S A_{eff}$. On the other hand if c_R is the average number of molecules per unit volume $N_{Vol} = c_R V = c_R H_{eff} A_{eff}$, where H_{eff} is the effective height of the scattering volume. Eq. (1) reduces to:

$$EF = \frac{I_{SERS} / \mu_M A_M \mu_S}{I_R / c_R H_{eff}}, \quad (2)$$

where the parameter H_{eff} , enables the connection between the 2D and 3D measurement. In the case of a complete coverage of the surface under illumination by CNCs, $\mu_M A_M$ is 1, and

$$EF = \frac{I_{SERS}}{I_R} f_p c_R H_{eff}, \quad (3)$$

Solid MBT ($\sim 53 \cdot 10^{20}$ molecules per cm^3) was used for the evaluation of I_R . H_{eff} was measured ($34 \mu\text{m}$) according with the procedure described in Cai *et al.* [W.B. Cai, B. Ren, X.Q. Li, C.X. She, F.M. Liu, X.W. Cai, *Surf. Sci.*, 1998, **406**, 9-23]. f_p was assumed = $0.19 \text{ nm}^2/\text{molecule}$ according to Rycenga *et al.* [M. Rycenga, X.H. Xia, C.H. Moran, F. Zhou, D. Qin, Z.Y. Li, Y.A. Xia, *Angew. Chem. Int. Edit.*, 2011, **50**, 5473-547]. In our experimental conditions, we measured a SERS signal ~ 100 times larger than the Raman one (Fig. S4), therefore we estimated an $EF \sim 10^6$.

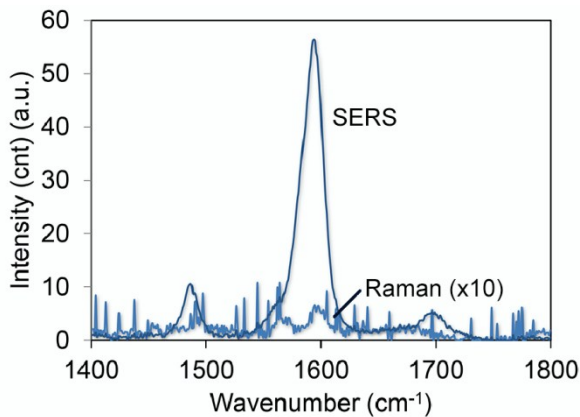


Fig. S4. Comparison between the 1594 cm^{-1} Raman and SERS bands of MBT.

Finite Element Method modeling

Simulation of the electric field has been performed using a finite element method (FEM). We realized our finite element models using the commercial software Comsol Multiphysics 4.4 in the scattering mode of the wave-optics-module to solve the Helmholtz equation. By normalizing the incident electric field we can observe the local field enhancement factor directly in form of the normalized electric field.

Our geometry is composed of several gold concave nanocubes with 100 nm size surrounded by air. We have considered three different mutual positions of the CNCs that are the most representative of the actual nanoparticle assembly as shown in the TEM images of Fig. 3. This choice represents a compromise between calculation domain size and solving time. The gold-to-gold gap distance is set to 1 and 0 nm for the face-to-face and face-to-corner configurations, respectively. The metal is described through its measured dielectric function [P.B. Johnson & R.W. Christy, *Phys. Rev. B*, 1972, **6**, 4370-4379]. The domains are delimited by perfectly matched layers (PML) in order to reach perfect absorption at the outer boundaries. All the simulation are done in 3D and the incident field is assumed to be an electromagnetic plane wave with linear polarization and 639 nm wavelength. Our experimental setup is with light at normal incidence onto the layer of nanocubes (light propagating along the z axis) and polarization along the y direction (see Fig. 4).

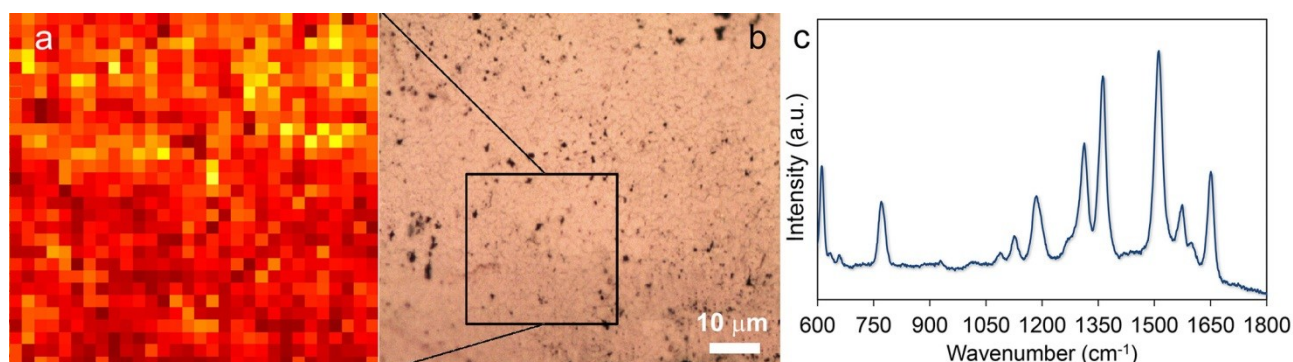


Fig. S5. False-color map (a) obtained by plotting the intensity of the 1511 cm⁻¹ Raman band of SERS spectra of Rhodamine 6G (a representative SERS spectrum is visualized in (c)) measured over a 30×30 μm² area with a resolution of 1×1 μm² of a CNCs-PDMS substrate as identified in the back-reflection image (b). The sample was prepared as described in the Methods section for protein samples and schematized in Fig. 1. A solution of Rhodamine 6G 1 10⁻⁶ M was used for the measurement.

Table S1. Assignment of Raman bands in the SERS spectra of insulin and cyt c shown in Fig. 5

protein	Raman shift (cm ⁻¹)	Raman band assignment	protein	Raman shift (cm ⁻¹)	Raman band assignment
Insulin	1642	Amide I	Cyt c	1633	ν ₁₀ , B _{1g} of heme
	1450	-CH ₂ deformation mode		1555	Trp
	1365	-CH deformation mode		1540	ν ₁₁ , B _{1g} of heme
	1385	-CH deformation mode		1447	CH ₂ deformation mode
	1270	Amide III		1370	ν ₄ , A _{1g} of heme
	1208	Phe		1366	ν ₄ , A _{1g} of heme
	1181	Tyr		1240	Amide III
	1030	Ring breathing mode Phe		1164	ν ₃₀ , B _{2g} of heme
	1003	Ring breathing mode Phe		1124	ν ₂₂ , A _{2g} of heme
	950	C-C stretching mode		1030	Ring breathing mode Phe
	866	Stretching and ring breathing mode Tyr		1000	Ring breathing mode Phe
	830	Stretching and ring breathing mode Tyr		860	Stretching and ring breathing mode Tyr
624	Phe	840	Stretching and ring breathing mode Tyr		

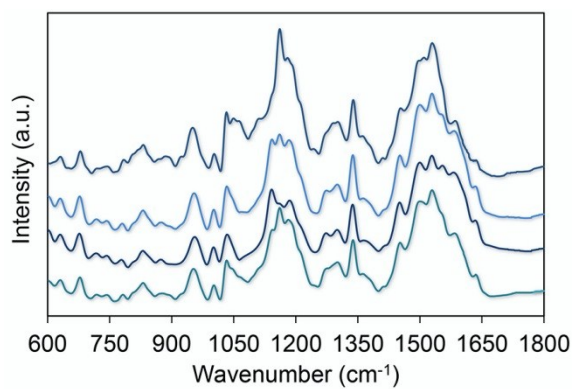


Fig. S6. Examples of SERS spectra of insulin taken from random locations of a CNCs-PDMS substrate.